Proceedings of the 2005 IEEE/ASME
International Conference on Advanced Intelligent Mechatronics
Monterey, California, USA, 24-28 July, 2005

Balancing 3D Objects with Rolling Constraint by Redundant Manipulator

S. Murat Yeşiloğlu
smy@ieee.org

Hakan Temeltaş
temeltas@elk.itu.edu.tr

Department of Electrical Engineering
Istanbul Technical University
34469 Istanbul, Turkey

Okyay Kaynak
kaynak@boun.edu.tr

Department of Electrical & Electronic Engineering
Bogazici University
80815 Istanbul, Turkey

***Abstract*— A novel methodology is presented for a practical problem of balancing a round object about its contact point posing pure rolling constraint at the tip of a redundant manipulator. Two-layer controller, the objective of the first of which is to balance the object as long as the manipulator stays in a singularity-free predefined task-space, is designed. We call that a "static balance." At the second layer, the contact point of the balanced object is aimed at repositioning at a close neighborhood of an, also predefined, conceptual center of task space where the dynamic manipulability is the greatest. We call this transition a "dynamic balance." In order to achieve the dynamic balance, one needs to disturb the static balance in a controlled manner. We, then, introduce the concept of an "equilibria cone" formed by the collection of static and dynamic equilibria.**

I. INTRODUCTION

Pure rolling constraint introduces nonholonomy which poses a challenge in getting the equation of motion of the system. Nonholonomic systems have been extensively studied for the last few decades. The work by Li and Canny [6] and the references therein can be considered as the milestones of this area of interest by early 90s. Iannitti and Lynch's research [4] constitutes a more recent work on not only nonholonomic systems but also underactuated ones.

Underactuation may arise when a manipulator includes at least one passive joint which is either a free joint where torque propagating along the axis of rotation is only due to friction, or a flexible joint which has passive elements introducing stiffness and damping. In this regard, free flying platform can be considered as linked to a fixed base by six DOF free joints with no friction as modeled in [10]. Dynamics of underactuated cooperating manipulators and their control is certainly a challenging research area. Ortega *et al.* [7] presented an energy based control algorithm for such systems. These type of studies usually take an inverted pendulum as a benchmark problem.

Spherical inverted pendulum has been studied by several researchers. To name just a few, Hoshino *et al.* [3] who demonstrated hand-over of 3D pendulum and Kajita *et al.* [5] who applied it to biped walking can be mentioned. Rolling contacts have been studied mostly under the context of dextrous manipulation. For example, control of Rolling contacts in multi-arm manipulation has been studied by Paljug *et al.* [8], Cole *et al.* [1], Deo and Walker [2].

In this paper, we are presenting a novel approach for a practical problem of balancing a round object about its contact point posing pure rolling constraint at the tip of a redundant manipulator. One may consider the problem posed here as a 3D inverted pendulum problem. On the other hand it is different from classical 3D pendulum as studied, for example, in [9] in the sense that no stable equilibrium exist in our problem.

The main contribution of this paper lies in the two-layer design of the controller. The objective of the first controller is to balance the object as long as the manipulator stays in a singularity-free predefined task-space. We call that a "static balance." At the second layer, the contact point of the balanced object is aimed at repositioning at a close neighborhood of an, also predefined, conceptual center of task space where the dynamic manipulability is the greatest. We call this transition a "dynamic balance." In order to achieve the dynamic balance, one needs to disturb the static balance in a controlled manner. We, then, introduce the concept of an "equilibria cone" formed by the collection of static and dynamic equilibria.

The outline of the paper is as follows: In Section II, we present the dynamical models for an n-link serial manipulator and the object in the form of two rigid bodies with rolling constraint. Section III is the equilibria analysis where we introduce the concepts of *equilibria cone* and *spatial dipole*. Section IV is to explain two-layer control as well as the layer switching logic algorithm and, finally, Section V concludes the paper.

II. DYNAMICAL MODELING

A. Nomenclature

The algorithm presented here utilizes a basis-free vectorial representation. The body coordinate frame is denoted by O. Right subscript of a variable indicates the associated link. For example, O_3 is the body frame on the third link. Right subscript indicates the size when necessary. For example ${}_3I$ is the 3×3 identity matrix, ${}_5 0$ is the 5×5 zero matrix. h_k is a unit vector parallel to the axis of rotation of the joint at the kth link. This definition is done under the assumption, without loss of generality, that each link has one DOF joint. In the presence of multiple DOF joints this assumption can easily be removed by making h_k include one unit vector per column. H_k and θ_k are the spatial axis of motion and the joint angle for the aforementioned joint,

respectively. $\ell_{k,k+1}$ is a vector from O_k to O_{k+1}. The linear and angular velocity vectors with respect to the inertial frame which is chosen as the base frame, O_0, are v_k and ω_k. Spatial velocity and the spatial acceleration of the link are denoted as V_k and α_k and they are defined as $\begin{pmatrix} \omega_k^T & v_k^T \end{pmatrix}^T$ and $\begin{pmatrix} \dot{\omega}_k^T & \dot{v}_k^T \end{pmatrix}^T$,respectively, where ^{T} is the transpose operator. m_k is the mass and $\mathcal{I}_k$ is the inertia tensor at point O_k. $\ell_{k,c}$ is the vector from O_k to the links center of mass. Link forces and torques acting at O_k are denoted as f_k and τ_k. Link spatial force vector F_k is defined as $\begin{pmatrix} \tau_k^T & f_k^T \end{pmatrix}^T$. Finally, skew symmetric linear operator of vector cross product is denoted by *hat*, i.e, $\widehat{p} = \vec{p}\times$.

B. Serial Manipulator Dynamics

In this section equation of motion will be derived for a serial manipulator. Angular and linear link velocities of the manipulator with respect to its base frame, propagate from link $k-1$ to link k as follows:

$$V_k = \phi_{k,k-1} V_{k-1} + H_k \dot{q}_k$$

where

$$\phi_{k,k-1} = \begin{bmatrix} {}_3I & {}_30 \\ -\widehat{\ell}_{k-1,k} & {}_3I \end{bmatrix}$$

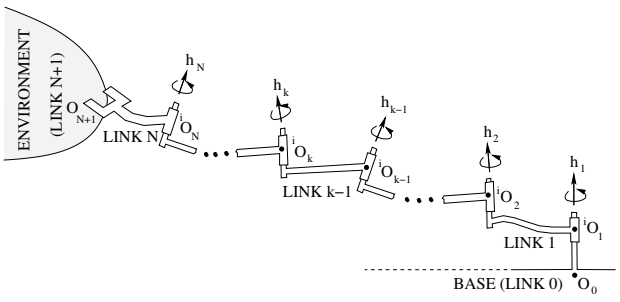

Fig. 1. N-link serial manipulator

$\phi_{k,k-1}$ is a linear operator that translates velocities from O_{k-1} to O_k and called the "propagation operator." Velocity vector, propagation operator and joint axes matrix are written as:

$$V = \begin{bmatrix} V_1 \\ V_2 \\ \vdots \\ V_n \end{bmatrix} \qquad V \in \Re^{6n\times 1}$$

$$\phi = \begin{bmatrix} {}_6I & {}_60 & \cdots & {}_60 \\ \phi_{2,1} & {}_6I & \cdots & {}_60 \\ \vdots & \vdots & \ddots & \vdots \\ \phi_{n,1} & \phi_{n,2} & \cdots & {}_6I \end{bmatrix} \qquad \phi \in \Re^{6n\times 6n}$$

$$H = \begin{bmatrix} H_1 & & & 0 \\ & H_2 & & \\ & & \ddots & \\ 0 & & & H_n \end{bmatrix} \qquad H \in \Re^{6n\times n}$$

where n is the number of DOF. Based on these definitions, the link velocities are obtained as follows:

$$V = \phi H \dot{q} \tag{1}$$

$\sigma_t = \begin{bmatrix} {}_60 & \cdots & \phi_{n,n-1} \end{bmatrix}$, the tip propagation operator, yields Jacobian by premultiplying both sides of (1)

$$V_t = \mathcal{J}\dot{q} \tag{2}$$

where,

$$\mathcal{J} \triangleq \sigma_t \phi H$$

The derivative of (1) provides the link accelerations:

$$\alpha = \phi(H\ddot{q} + a) \tag{3}$$

where a is the the stacked up bias acceleration term. Bias acceleration of link k is defined as

$$a_k = \begin{bmatrix} (\widehat{\omega}_{k-1}\omega_k)^T & (\widehat{\omega}_{k-1}^2 \ell_{k-1,k})^T \end{bmatrix}^T \tag{4}$$

Spatial forces are calculated from tip to base. Therefore, ϕ^T, in this case, becomes the propagation operator.

$$f = \phi^T(M\alpha + b + \sigma_t^T F_t) \tag{5}$$

where F_t is the tip forces and b is the spatial bias forces. The definition of spatial bias forces acting on link k is given as

$$b_k = \begin{bmatrix} (\widehat{\omega}_k \mathcal{I}_k \omega_k)^T & (m_k \widehat{\omega}_k^2 \ell_{k,c})^T \end{bmatrix}^T$$

We obtain the applied torques if we project the spatial force vector given in (5) onto the axis of motion.

$$\mathcal{T} = H^T f \tag{6}$$

Substituting (5) in (6), we get the equation of motion as

$$\mathcal{T} = \mathcal{M}\ddot{q} + C + \mathcal{J}^T F_t \tag{7}$$

where

$$\mathcal{M} \triangleq H^T \phi^T M \phi H$$

$$C \triangleq H^T \phi^T M \phi a + H^T \phi^T b$$

Hence, forward dynamical model is obtained as

$$\ddot{q} = \mathcal{M}^{-1}(\bar{\mathcal{T}} - \mathcal{J}^T F_t) \tag{8}$$

where

$$\bar{\mathcal{T}} \triangleq \mathcal{T} - C$$

C. Pure Rolling

In this section, velocity and acceleration analysis of a ball rolling on another ball is studied. Without loss of generality we consider that each ball has a concentrated point mass at its center of mass. Let point A and B be the mass center of the balls, point C be the point of contact, and r1 and r2 be the radius of the balls as shown in Figure 2. It is assumed that the ball with radius r_1 is non-rotating. Figure 2 also displays the basis vectors for non-rotating ball as $(\vec{x}_1, \vec{y}_1, \vec{z}_1)$, and for the point of contact as $(\vec{x}_2, \vec{y}_2, \vec{z}_2)$, and the angles θ, ϕ, β which are defined as the fall angle, the swing angle, and the angle of rotation about its axis of symmetry passing through

the contact point, respectively. It should be pointed out that, as long as the system is not subject to an external torque along $\vec{z}_2$, then $\dot{\beta}$ will remain zero. Since it will be the case here, we will ignore the effect of the derivatives of β to the dynamic model.

Let us first start with the constraint of nonholonomy exist at point C due to pure rolling, in other words, no-sliding.

$$\vec{v}_c + r_1(\dot{\theta}\vec{x}_2 + \dot{\phi}\vec{z}_1) \times \vec{z}_2 = \vec{v}_t \tag{9}$$

where $\vec{v}_t$ and $\vec{v}_c$ are the linear velocities of point T and point C, respectively.

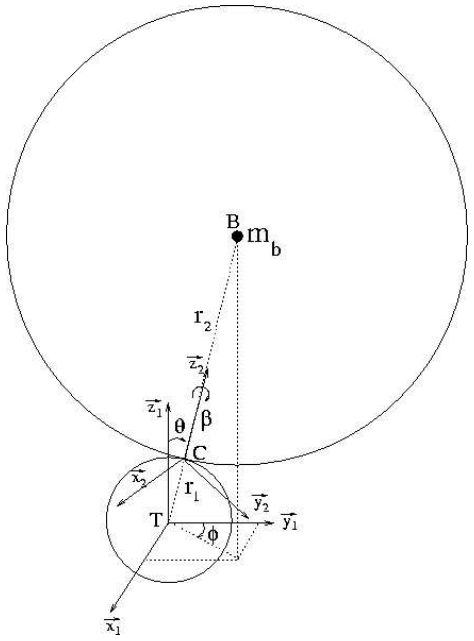

Fig. 2. Two balls with pure rolling constraint

The linear and angular velocities are written as follows:

$$\begin{aligned}
\vec{\omega}_c &= -\dot{\theta}\vec{x}_2 - \dot{\phi}\vec{z}_1 \\
&= -\dot{\theta}\vec{x}_2 + \dot{\phi}sin\theta\vec{y}_2 - \dot{\phi}cos\theta\vec{z}_2 \qquad (10)\\
\vec{\omega}_b &= \frac{r}{r_2}\vec{\omega}_c \qquad (11)\\
\vec{v}_b &= r\vec{\omega}_c \times \vec{z}_2 + \vec{v}_t \\
&= r(\dot{\phi}sin\theta\vec{x}_2 + \dot{\theta}\vec{y}_2) + \vec{v}_t \qquad (12)
\end{aligned}$$

where $r = r_1 + r_2$. Taking time derivative of 12 gives us the linear acceleration of the center of mass of ball B.

$$\dot{v}_b = r\begin{bmatrix} \ddot{\phi}sin\theta + 2\dot{\theta}\dot{\phi}cos\theta \\ \ddot{\theta} - \dot{\phi}^2 sin\theta cos\theta \\ -\dot{\theta}^2 - \dot{\phi}^2 sin^2\theta \end{bmatrix} + \dot{v}_t \tag{13}$$

represented in $(\vec{x}_2, \vec{y}_2, \vec{z}_2)$ frame. Taking time derivative of 11 gives us the angular acceleration of ball B.

$$\dot{\omega}_b = \frac{r}{r_2}\begin{bmatrix} -\ddot{\theta} + \dot{\phi}^2 sin\theta cos\theta \\ \ddot{\phi}sin\theta + \dot{\theta}\dot{\phi}cos\theta \\ -\ddot{\phi}cos\theta + (\dot{\theta} - \dot{\phi}cos\theta)\dot{\phi}sin\theta \end{bmatrix} \tag{14}$$

also represented in $(\vec{x}_2, \vec{y}_2, \vec{z}_2)$ frame.

Looking at the equations given above, for the sake of better understanding the system, we can make an analogy between the two-ball-rolling system and what we call *spatial dipole* as pictured in Figure 3, where m is the mass, and $\mathcal{I}$ is the inertia of the ball with radius r_2 defined at the contact point C, and F_t is the external force applied at the center of mass of the ball with radius r_1.

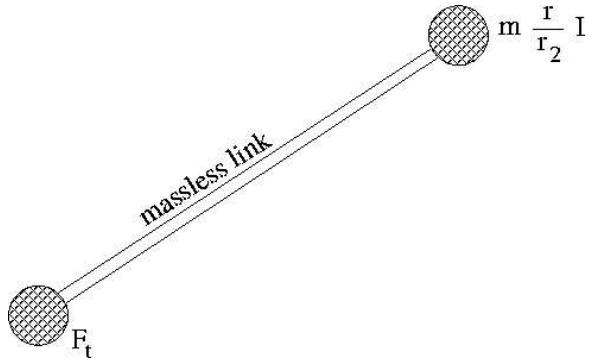

Fig. 3. Spatial dipole

Considering the spatial dipole characteristic as depicted in Figure 3, two-ball-rolling problem resembles, in a way, the 3D inverted pendulum problem. This statement is true only around some neighborhood of the well-known unstable equilibrium state of the pendulum. This is because not only that there is no hanging state which is the stable equilibrium of pendulums, but also the given spatial dipole characteristic is only valid as long as the two balls are in contact.

III. EQUILIBRIA ANALYSIS

In this section, we bring the concept of "carrying an inverted pendulum" from one point to another. Imagine that you are holding a long inverted pendulum in balance at your fingertip. If you want to move your hand to another point while keeping the pendulum in balance, you need to disturb the pendulum from equilibrium point in an opposite direction of where you want to take your hand to in a careful way and then accelerate your hand towards that final point and, once you are about to get there, accelerate further and bring the pendulum back into the equilibrium. This is essentially the main idea presented here. Let us start this analysis by the following definitions.

Definition 1: *Holding vector* is the displacement from the contact point to the center of mass of the object as shown in Figure 4.

Definition 2: The object is said to be at an *equilibrium* if the holding vector stands still while staying in the task-space provided that there is no external disturbance introduced to the system.

Definition 3: *Static balance* occurs when the system is at an equilibrium such that the holding vector is parallel with the gravitational vector (inertial vertical).

Definition 4: *Dynamic balance* occurs when the system is at an equilibrium such that the holding vector is not parallel with the gravitational vector.

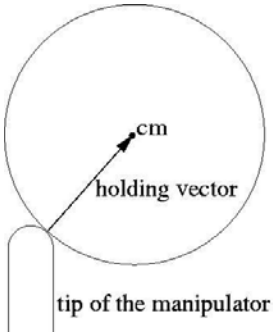

Fig. 4. Holding vector

Based on the definitions made above, we can now state the following proposition:

Proposition 1: *Equilibria cone* represents all admissible holding vectors in static and dynamic balance.

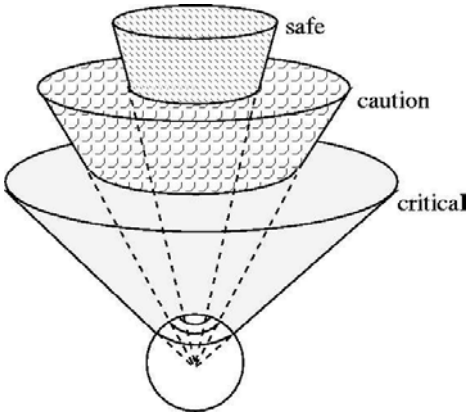

Fig. 5. Three segment equilibria cone

Equilibria cone is essentially the friction cone introduced with a segmentation property as proposed next.

Proposition 2: Equilibria cone consists of equally spaced three segments: safe, caution and critical.

The use and the details of segments introduced in Proposition 2 and shown in Figure 5 will be given in the second layer controller part of the following section.

IV. TWO-LAYER CONTROL

Before going into the control issues, let us first define the task-space in which tip of the manipulator holding the ball is desired to remain. In order to avoid singularities, task-space is not chosen as the complete work-space. Rather, conservative measures are taken in selection of the task-space so that manipulability is satisfactory throughout the defined space. Joint-space analysis is also considered to make sure the manipulation in task-space can be achieved as singularity-free and away from the joint mechanical limits. Furthermore, a single point where the manipulability is the greatest in this task-space is labeled as the *conceptual center of task-space* (CCTS).

The control objective is to keep the ball in static balance at a close neighborhood of the CCTS. Therefore, we need to divide this problem into two subproblems:

- bring the ball in static balance
- when the ball is in static balance, check how far it is from the CCTS. If this distance called *deviation norm* is larger than certain value, than switch to the dynamic balance mode and move to the CCTS.

The first and the latter subproblems as outlined above are the objectives of *the first layer controller* and *the second layer controller*, respectively, while the logic explained in the objective of the second layer controller is derived by so called *layer switching logic*. Figure 6 displays the high-level schematic of the controller, system and sensing interaction.

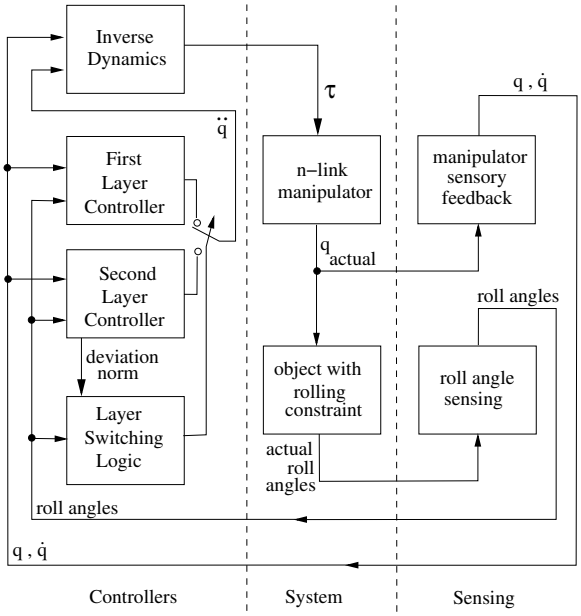

Fig. 6. High level schematic of the controller, system and sensing interaction

A. First Layer: Balancing

The Euler's law of motion gives us the equation the system has to obey as the following:

$$m_b r_2 \vec{z}_2 \times \dot{\vec{v}}_b = \mathcal{I}_b \dot{\vec{\omega}}_b \tag{15}$$

where m_b is the mass, $\mathcal{I}_b$ is the inertia of the ball.

Let say $\vec{v}_t$ has a representation of $[\dot{v}_{tx_2} \ \dot{v}_{ty_2} \ \dot{v}_{tz_2}]^T$ in $(\vec{x}_2, \vec{y}_2, \vec{z}_2)$ frame. Substituting equations 13 and 14 into 15, we get:

$$m_b r r_2 \begin{bmatrix} -\ddot{\theta} + \dot{\phi}^2 sin\theta cos\theta \\ \ddot{\phi} sin\theta + 2\dot{\theta}\dot{\phi} cos\theta \\ 0 \end{bmatrix} + m_b r_2 \begin{bmatrix} -\dot{v}_{ty_2} \\ \dot{v}_{tx_2} \\ 0 \end{bmatrix} = \frac{r\mathcal{I}_b}{r_2} \begin{bmatrix} -\ddot{\theta} + \dot{\phi}^2 sin\theta cos\theta \\ \ddot{\phi} sin\theta + \dot{\theta}\dot{\phi} cos\theta \\ -\ddot{\phi} cos\theta + (\dot{\theta} - \dot{\phi} cos\theta)\dot{\phi} sin\theta \end{bmatrix} \tag{16}$$

From equation 16, we find the required accelerations to keep the ball in static balance.

$$\dot{v}_{tx_2} = \frac{r\mathcal{I}_b - m_b r r_2^2}{m_b r_2^2}(\ddot{\phi} sin\theta + \dot{\theta}\dot{\phi} cos\theta) - r\dot{\theta}\dot{\phi} cos\theta \quad (17)$$

$$\dot{v}_{ty_2} = \frac{r\mathcal{I}_b - m_b r r_2^2}{m_b r_2^2}(\ddot{\theta} - \dot{\phi}^2 sin\theta cos\theta) \quad (18)$$

It is only logical here to set $\dot{v}_{tz_2} = 0$. Rotation matrix from frame $(\vec{x}_2, \vec{y}_2, \vec{z}_2)$ to frame $(\vec{x}_1, \vec{y}_1, \vec{z}_1)$ is

$$R = \begin{bmatrix} cos\phi & -cos\theta sin\phi & sin\theta sin\phi \\ sin\phi & cos\theta cos\phi & -sin\theta cos\phi \\ 0 & sin\theta & cos\theta \end{bmatrix} \quad (19)$$

Therefore, tip point accelerations represented in $(\vec{x}_1, \vec{y}_1, \vec{z}_1)$ frame becomes:

$$\dot{v}_t = \begin{bmatrix} \dot{v}_{tx_2} cos\phi - \dot{v}_{ty_2} cos\theta sin\phi \\ \dot{v}_{tx_2} sin\phi + \dot{v}_{ty_2} cos\theta cos\phi \\ \dot{v}_{ty_2} sin\theta \end{bmatrix} \quad (20)$$

B. Second Layer: Tracking

Here, "tracking" refers to bringing the contact point to a close neighborhood of conceptual center of task-space (CCTS). This is done in three phases in the following order:

- "disturb and wait" phase
- dynamic balance phase
- static balance phase

"Disturb and wait" phase:

First, the *deviation vector* is defined as the displacement from the tip of the manipulator to the CCTS.

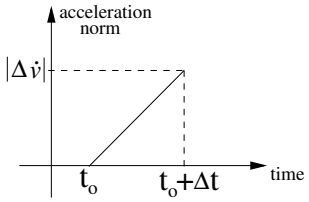

Fig. 7. Disturb phase

During the disturb phase, the tip of the manipulator moves towards the opposite direction of the deviation vector following ramp acceleration as shown in Figure 7. Both $\Delta\dot{v}$ and Δt are chosen small enough so that the static balance is not disturbed too much. After that we are at the "wait" part of this phase while the tip of the manipulator continues to move towards the opposite direction of the deviation vector at a constant linear velocity. Let φ be the absolute value of the angle between the holding vector and the deviation vector, and φ_o is that value during the static balance. Now, assign $\gamma = k \cdot mod(\varphi, \frac{\pi}{2})$. We "wait" until $\varphi = \varphi_o - \gamma$. In calculation of $\gamma, 0 < k < 1$ will be chosen such that at the time when $\varphi = \varphi_o - \gamma$, holding vector is in caution segment of the equilibrium cone, close to the critical segment boundary.

Dynamic balance phase:

Since $\dot{v}_{tz_2}$ term is not there in equation 16, we are free to choose it. Consequently, equation 20 becomes

$$\dot{v}_t = \begin{bmatrix} \dot{v}_{ax_2} cos\phi - \dot{v}_{ay_2} cos\theta sin\phi + \dot{v}_{az_2} sin\theta sin\phi \\ \dot{v}_{ax_2} sin\phi + \dot{v}_{ay_2} cos\theta cos\phi - \dot{v}_{az_2} sin\theta cos\phi \\ \dot{v}_{ay_2} sin\theta + \dot{v}_{az_2} cos\theta \end{bmatrix} \quad (21)$$

While $\dot{v}_{tx_2}$ and $\dot{v}_{ty_2}$ are calculated from 17 and 18, $\dot{v}_{az_2}$ is determined so that $\dot{v}_t$ is parallel with the deviation vector.

Static balance phase:

In order to maintain static balance, first layer controller is switched back.

C. Inverse Dynamics

Now, let us look at how the computed torque block in figure 6 works.

Since we want to keep the orientation of the tip point at its initial orientation, $\vec{\omega}_t = \vec{0}$. Hence, the spatial tip acceleration is $\dot{V}_t = [0\ 0\ 0\ \dot{v}_t^T]^T$. Taking time derivative of equation 2 yields

$$\dot{V}_t = \mathcal{J}\ddot{q} + \sigma_t \phi a + a_t \quad (22)$$

where a, a_t are the spatial bias accelerations as defined in equation 4. Please keep in mind that the manipulator in consideration here is a redundant manipulator and, hence, the joint-space to task-space mapping is an under-determined case. Since we are studying the system only in a singularity-free task space, the least square pseudo inverse of the Jacobian can be obtained.

$$\mathcal{J}^{\#} = \mathcal{J}^T(\mathcal{J}\mathcal{J}^T)^{-1} \quad (23)$$

Now we can calculate the joint accelerations as

$$\ddot{q} = \mathcal{J}^{\#}(\dot{V}_t - \sigma_t \phi a - a_t) \quad (24)$$

Joint torques are calculated from equation 7. Dynamic interaction between the ball and the manipulator is negligible on the manipulator side when compared the mass of the ball with that of manipulator. Therefore, F_t term in equation 7 can be ignored. On the other hand, one needs to keep in mind that inverse dynamics based control will be parameter sensitive unless a PD type inner feedback loop is introduced. Although such details as inner loop control is not shown in figure 6, the actual controller does include it.

D. Layer Switching Logic

In order to be able to decide when to switch from one layer to another layer controller, static balance has to be well defined. If roll angle θ is smaller than a small certain value (predefined) for a reasonable time (predefined), than we can conclude that the system is in static balance. Meanwhile, the layer switching logic box is being fed the Euler ($\mathcal{L}_2$) norm of deviation vector by the second layer controller. If this norm is larger than a certain value (predefined) while the system is in static balance, than the logic box calls for the second layer controller. When the second layer finishes phase 1 and phase 2 as explained before, then the logic box switches the first layer controller back on.

V. CONCLUSION

We have presented a mathematical model for an underactuated mechanical system subject to pure-rolling constraint. We developed a methodology for balancing and trajectory tracking of a ball as a 3D pendulum without stable equilibrium (hanging state) rolling on another ball. Pure

rolling constraint introduces nonholonomy which poses a challenge from modeling and control point of view. This paper contributed to the theoretical framework for the practical prablem of balancing an object with a convex-shaped non-sliding point contact with a convex-shaped tip of a manipulator.

REFERENCES

[1] A. Cole, J. Hauser, and S. Sastry. Kinematics and control of multifingered hands with rolling contact. *IEEE Transactions on Automatic Control*, 34(4):398–404, 1989.

[2] A. S. Deo and I. D. Walker. Dynamics and control of multiple cooperating manipulators with rolling contacts. *Journal of Robotic Systems*, 13(10):619–648, 1996.

[3] T. Hoshino, M. Hara, and K. Furuta. A new controller design scheme for cooperating manipulators – a reliable design approach. *Advanced Robotics*, 13(6):603–616, 2000.

[4] S. Iannitti and K.M. Lynch. Minimum control-switch motions for the snakeboard: A case study in kinematically controllable underactuated systems. *IEEE Transactions on Robotics*, 20(6):994–1006, December 2004.

[5] S. Kajita, F. Kanehiro, K. Kaneko, K. Fujiwara, K. Yokoi, and H. Hirukawa. A realtime pattern generator for biped walking. In *International conference on robotics & automation*, pages 31–37, Washington, DC, May 2002.

[6] Z. Li and J. Canny. Motion of two rigid bodies with rolling constraint. *IEEE Transactions on Robotics and Automation*, 6(1):62–72, February 1990.

[7] R. Ortega, M. Spong, F. Gomez-Estern, and Blankenstein G. Stabilization of a class of underactuated mechanical systems via interconnection and damping assignment. *IEEE Transactions on Automatic Control*, 47(8):1218–1233, August 2002.

[8] E. Paljug, X. Yun, and V. Kumar. Control of rolling contacts in multi-arm manipulation. *IEEE Transactions on Robotics and Automation*, 10(4):441–451, August 1994.

[9] J. Shen, A.K. Sanyal, N.A. Chaturvedi, D. Bernstein, and H. McClamroch. Dynamics and control of a 3d pendulum. In *Proc. of 43rd IEEE Conference on Decision and Control*, pages 323–328, Paradise Island, Bahamas, 2004.

[10] S. M. Yesiloglu and H. Temeltas. High performance algorithm on the dynamics of general underactuated cooperating manipulators. In *Proceedings of the IEEE International Conference on Mechatronics & Robotics*, pages 531–536, Aachen, Germany, September 2004.